# Title: Multi-mode Combustion Process Monitoring on a Pulverised Fuel Combustion Test Facility based on Flame Imaging and Random Weight Network Techniques

**Authors**: Xiaojing Bai[1, 2], *Gang Lu[2], Md Moinul Hossain[2], Janos Szuhánszki[3], Syed Sheraz Daood[3], William Nimmo[3], Yong Yan[2], Mohamed Pourkashanian[3]

**Address:** [1.] School of Control and Computer Engineering,
North China Electric Power University,
Beijing, 102206, China

[2.] School of Engineering and Digital Arts,
University of Kent,
Canterbury,
Kent CT2 7NT, UK

[3.] Energy 2050 Group,
Department of Mechanical Engineering,
University of Sheffield,
Sheffield, S10 2TN, UK
Email: xb9@kent.ac.uk, g.lu@kent.ac.uk, m.hossain@kent.ac.uk,
j.szuhanszki@sheffield.ac.uk, s.daood@sheffield.ac.uk, w.nimmo@sheffield.ac.uk,
y.yan@kent.ac.uk, m.pourkashanian@sheffield.ac.uk

## ABSTRACT

Combustion systems need to be operated under a range of different conditions to meet fluctuating energy demands. Reliable monitoring of the combustion process is crucial for combustion control and optimisation under such variable conditions. In this paper, a monitoring method for variable combustion conditions is proposed by combining digital imaging, PCA-RWN (Principal Component Analysis and Random Weight Network) techniques. Based on flame images acquired using a digital imaging system, the mean intensity values of RGB (Red, Green, and Blue) image components and texture descriptors computed based on the grey-level co-occurrence matrix are used as the colour and texture features of flame images. These features are treated as the input variables of the proposed PCA-RWN model for multi-mode process monitoring. In the proposed model, the PCA is used to extract the principal component features of input vectors. By establishing the RWN model for an appropriate principal component subspace, the computing load of recognising combustion operation conditions is significantly reduced. In addition, Hotelling's $T^2$ and SPE (Squared Prediction Error) statistics of the corresponding operation conditions are calculated to identify the abnormalities of the combustion. The proposed approach is evaluated using flame image datasets obtained on a 250 $kW_{th}$ air- and oxy-fuel Combustion Test Facility. Variable operation conditions were achieved by changing the primary air and SA/TA (Secondary Air to Territory Air) splits. The results demonstrate that, for the operation conditions examined, the condition recognition success rate of the proposed PCA-RWN model is over 91%, which outperforms other machine learning classifiers with a reduced training time. The results also show that the abnormal conditions exhibit different oscillation frequencies from the normal conditions, and the $T^2$ and SPE statistics are capable of detecting such abnormalities.



**Keywords:** fossil fuel combustion, multi-mode process monitoring, flame image, principal components analysis, random weight network.

## 1. Introduction

In power generation industries, boilers are required to operate under optimised conditions to maintain high combustion efficiency and low emissions. Abnormal combustion states caused by drifts or faults in a combustion system can result in not only reduced efficiency and increased emissions but also enormous negative impact on the health of the system. The recent trend of using a variety of fuels, including low-quality coals, coal blends, and co-firing biomass and coal, has further exacerbated this issue [1, 2]. Hence, the combustion process monitoring has received considerable attention.

Flame imaging incorporating soft-computing algorithms is considered to be a promising technical approach to monitoring the combustion process as it provides the operators with reliable, 2-D (two-dimensional) measurements about the furnace [3]. Several studies have been carried out for combustion process monitoring based on flame imaging techniques. Sun et al. [1] applied KPCA (Kernel Principal Component Analysis) for the diagnosis of abnormal operation conditions on a heavy oil-fired combustion test facility. Chen et al. [4] proposed an online predictive technique for furnace performance monitoring based on dynamic imaging and the combination of Hidden Markov Model and multiway PCA. Li et al. [3] and Chen et al. [5] constructed an extreme learning machine using flame image features to recognise the burning state (i.e., over burning, normal burning, or under burning) in a rotary kiln. Wang and Ren [6] also suggested a flame imaging and machine learning based method for recognising combustion conditions in a pulverised coal-fired rotary kiln. These methods are designed for detecting the process under individual operation conditions, i.e., the single-mode process where only a normal condition is considered.

However, modern combustion systems often operate under variable conditions (i.e., multi-mode process) according to the demand for energy. This means that the combustion process can be normal or abnormal under each condition. The single-mode process monitoring method will fail to distinguish abnormalities from normal deviations in a multi-mode process. Therefore, multi-mode process monitoring techniques are required to recognise reliably the operation condition and assess the state (normal or abnormal) of the process under variable operation conditions. Existing multi-mode monitoring approaches can be divided into three categories, i.e. global-model, adaptive-model and local-model. The global-model builds generally an uniform model for all operations to achieve the process monitoring. Shang et al. [7] used slow feature analysis and classical statistics for the concurrent monitoring of operation condition deviations and process dynamics anomalies. Ma et al. [8] and Wang et al. [9] employed the standardisation method to transform the multi-mode data to an uniform distribution, which then incorporates a PCA model for the fault detection of multi-mode processes. Whereas, describing all kinds of operation conditions through an uniform model is challenging, especially for the conditions with significant distinction. The adaptive model adjusts model parameters adaptively and updates the model with operation conditions [10, 11]. Lee et al. [10] extracted process knowledge based on if-then rules for detecting the change in operation conditions. Ge and Song [12] proposed an adaptive local model approach to online monitoring of nonlinear multiple mode processes with non-Gaussian information. In an adaptive model, the modelling update speed is essential and the monitoring performance is mainly determined by the model selection. In a multi-mode combustion process, however, some conditions show significant differences and the dynamic behaviours of flames lead to the complexity of the features extracted from flame images. It is thus very difficult to build appropriate global or adaptive models to achieve multi-mode process monitoring in a combustion system. The local model recognises the operation conditions using clustering methods and builds multiple models for each operation condition to assess the state. Feital et al. [13] presented a multimodal modelling and monitoring method for multivariate

multimodal processes based on the maximum likelihood PCA and a component-wise identification of operating modes. Yang et al. [14] proposed an aligned mixture probabilistic PCA to exploit within-mode correlations for the fault detection of multi-mode chemical processes. However, in flame imaging based combustion monitoring, the features extracted from flame images, which are considered as input variables, suffer from various noises from either the imaging system or the combustion process as well as abnormalities in the combustion process. As a consequence, it is challenging to determine the most suitable model for every new sample using the existing multi-mode monitoring approaches. Appropriate methods are therefore required for recognising the combustion operation conditions and detecting the combustion state.

In this paper, a flame imaging and PCA-RWN (PCA-Random Weight Network) based multi-mode technique is proposed to achieve combustion process monitoring under variable conditions. In the PCA-RWN model, a global PCA model for all operation conditions is built to extract the features from flame images, and an RWN model is constructed for recognising the operation conditions. Cross-validation is used to select the optimal number of principal components of the PCA and the hidden nodes of the RWN. The PCA-RWN model can reduce significantly the computing overhead of the RWN model. This is achieved by dividing the inputs of the RWN model into a PCA based feature space and the optimised number of principal components are adaptively selected to obtain the optimal recognition performance of operation conditions. Following the recognition of the operation condition, Hotelling's $T^2$ and SPE are used to detect the combustion abnormalities. The performance of the proposed technique is evaluated using flame images obtained on the 250 $kW_{th}$ air- and oxy-fuel CTF (Combustion Test Facility) at the UKCCSRC PACT (Pilot Scale Advanced Capture Technology) Core Facilities. Experimental results show that the proposed PCA-RWN based multi-mode process monitoring

method is feasible and effective for detecting the abnormalities of combustion processes under variable operations.

## 2. Methodology

### *2.1 Overall strategy*

Fig. 1 shows the scheme of the PCA-RWN based multi-mode combustion process monitoring method. The scheme has three main steps, i.e. feature calculation, feature extraction and process monitoring. Firstly, flame images are pre-processed to reduce the noises by employing a moving average filter. Filtered flame images are then used to compute the colour and texture features of the flame. Secondly, the PCA model is built to extract the useful feature variables from the calculated features of the filtered flame images. Principal component feature spaces with different numbers of principal components are then considered, and the extracted features with various dimensions are taken as the inputs of the RWN model to perform the fitting tasks. Subsequently, processing is taken to search for the minimum-error and to select the well-trained RWN with the optimal numbers of principal components and hidden nodes according to the fitting errors of the RWN model. By using the certain well-trained PCA-RWN, the combustion operation condition of the targeted test flame image is recognised, and multiple variable statistics indices, the $T^2$ and SPE (Squared Prediction Error), are finally calculated to identify the state.

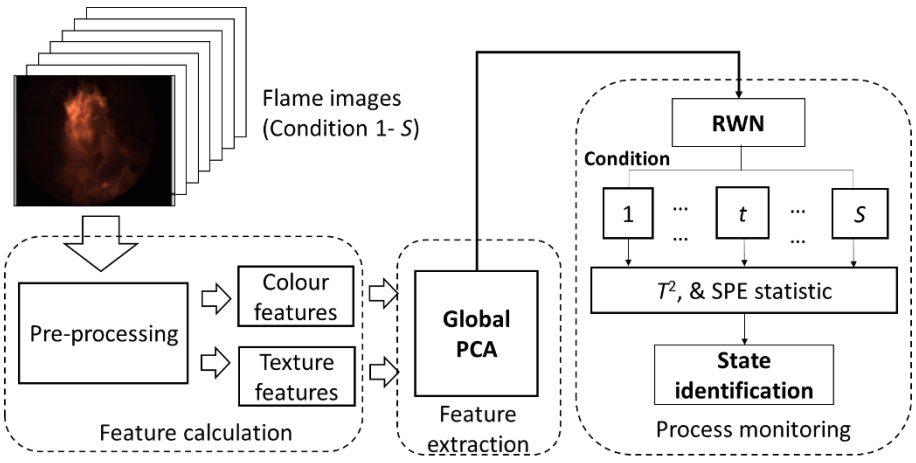

Fig. 1 Scheme of PCA-RWN based multi-mode combustion process monitoring.

*2.2 Principal component analysis based feature extraction*

In general, as one essential step in the flame visualisation, flame images are segmented to identify the flame regions using edge detection or other grey-level threshold methods [15]. Regarding coal combustion under variable operation conditions, it is very challenging to allocate precisely the boundary of the flame region in a very short time due to the dynamic nature of the flame. The inaccurate segmentation of the flame region will lead to inaccurate feature extraction, and thus poor monitoring performance. In this study, therefore, the colour and texture features of flame images are computed without any prior image segmentation. In this way, the adverse effects of flame image processing are significantly reduced. The colour features and texture features are calculated as follows:

**Step 1.** Original flame images need to be filtered to reduce noise using a moving average filter [16]. The *i*-th filtered image, $\bar{\boldsymbol{I}}_i$, is represented as,

$$\bar{\boldsymbol{I}}_i = \frac{1}{w}\sum_{\tau=0}^{w-1}\boldsymbol{I}_{i-\tau} \quad , \tag{1}$$

where $\boldsymbol{I}_i$ represents the corresponding original flame image to the *i*-th filtered image. *w* is the number of images used in the moving average filter. In this study, *w* is selected as 10 based on a number of trials to ensure that noise in the images is effectively removed within the period of acceptable processing time.

**Step 2.** Assume colour features $f_r$, $f_g$ and $f_b$ are the mean intensity values of R (Red), G (Green), and B (Blue) images of the flame, respectively, the colour features are then calculated as,

$$f_c = \sum_{p=1}^{u}\sum_{q=1}^{v}\boldsymbol{i}_c(p,q)/u/v,\ c\in\{r,\ g,\ b\} \quad , \tag{2}$$

where $\boldsymbol{i}_r$, $\boldsymbol{i}_g$, and $\boldsymbol{i}_b$ stand for the intensity matrices of R, G, and B images, respectively. $u$ and $v$ are the height and width of the flame image, respectively. $p$ and $q$ indicate the pixel position in the flame image ($p=1, 2,..., u$, and $q=1, 2,..., v$), respectively.

**Step 3.** A total of 14 texture features based on the grey-level co-occurrence matrix proposed by Haralick et al. [17] are introduced, i.e., energy ($f_1$), contrast ($f_2$), correlation ($f_3$), sum of variance squares ($f_4$), inverse difference moment ($f_5$), sum average ($f_6$), sum variance ($f_7$), sum entropy ($f_8$), entropy ($f_9$), difference variance ($f_{10}$), difference entropy ($f_{11}$), information measure of correlation I ($f_{12}$), information measure of correlation II ($f_{13}$), and the maximum probability ($f_{14}$). These features represent the texture characteristics of flame images and have been found effective in flame classification [6, 18]. A more detailed description and associated calculation of the grey-level co-occurrence matrix based texture features can be found in [6] and [17].

Therefore, for a filtered flame image, the feature vector of $i$-th flame image, $\boldsymbol{d}_i$, is defined as,

$$\boldsymbol{d}_i = [f_r^{(i)}, f_g^{(i)}, f_b^{(i)}, f_1^{(i)}, ..., f_{14}^{(i)}] \in \mathbb{R}^N,\ N = 17. \tag{3}$$

The feature matrix for the $s$-th ($s=1, 2,..., S$, $S$ is the number of total conditions) condition, $\boldsymbol{D}_s$, is denoted as,

$$\boldsymbol{D}_s = [\boldsymbol{d}_{s1}^{\mathrm{T}}, \boldsymbol{d}_{s2}^{\mathrm{T}}, ..., \boldsymbol{d}_{sm_s}^{\mathrm{T}}], \tag{4}$$

where $m_s$ stands for the sample number under the $s$ condition. As a multivariate statistic model, the PCA model is employed to project the feature space of flame images into two orthogonal subspaces and reduce the dimension of feature vectors. Based on the vectors of image features shown in (3) and (4), the PCA model is described as,

$$\boldsymbol{X}\boldsymbol{P}' + \boldsymbol{E} = \boldsymbol{D} := [\boldsymbol{D}_1, \boldsymbol{D}_2, ..., \boldsymbol{D}_S]^{\mathrm{T}}, \tag{5}$$

where $\boldsymbol{X}$ stands for the score matrix, $\boldsymbol{P}$ the loading matrix, and $\boldsymbol{E}$ the residual matrix. The singular value decomposition of the correlation matrix of $\boldsymbol{D}$ [19], i.e. $\Xi$, is given by

$$\boldsymbol{U}\Lambda\boldsymbol{U}^{\mathrm{T}} = \Xi := \boldsymbol{D}\boldsymbol{D}^{\mathrm{T}}/m, \tag{6}$$

where $\boldsymbol{U}=[\boldsymbol{u}_1, \boldsymbol{u}_2, \cdots, \boldsymbol{u}_N]$ represents an $N \times N$ unitary matrix, $\boldsymbol{\Lambda}$ is the diagonal matrix of eigenvalues, $m=m_1+m_2+\ldots+m_s$. If the number of principal components is $n$, the loading matrix $\boldsymbol{P}:=\boldsymbol{P}_n$ is represented as the matrix consisting of the front $n$ eigenvectors, marked as $\boldsymbol{P}_n=[\boldsymbol{u}_1, \boldsymbol{u}_2, \cdots, \boldsymbol{u}_n]$. The principal component information, i.e. the score matrix $\boldsymbol{X}$, of $\boldsymbol{D}$ is calculated as,

$$\boldsymbol{X} = \boldsymbol{D}\boldsymbol{P}_n . \tag{7}$$

*2.3 Random weight network (RWN)*

A RWN was originally proposed in [20, 21], where it was named as Extreme Learning Machine, for training a Feed-forward Neural Network, especially a Single-Hidden-Layer Feed-forward Network. In the RWN, parts of the hidden-node parameters are randomly generated based on probability distributions rather than well-tuned according to learning algorithms [22, 23]. The RWN has shown prominent performances at a much faster learning speed with less human intervention in both theory and applications.

Let $\{\boldsymbol{x}_i, \boldsymbol{y}_i\}_{i=1}^m$ be the given training samples with inputs $\boldsymbol{x}_i \in \mathbb{R}^n$ and target outputs $\boldsymbol{y}_i \in \mathbb{R}^M$, where $M$ is the dimension of the output. Let $\boldsymbol{o}_i \in \mathbb{R}^M$ denote the real outputs of $i$-th training sample in RWN model. The random weight network model is represented as,

$$\sum_{j=1}^{L} \boldsymbol{\beta}_j \Phi(\boldsymbol{\omega}_j \boldsymbol{x}_i^{\mathrm{T}} + \boldsymbol{b}_j) = \boldsymbol{o}_i, \ i = 1, 2, \cdots, m , \tag{8}$$

where $L$ stands for the number of hidden nodes in the RWN model, $\Phi(.)$ stands for the activation function, $\boldsymbol{\omega}_j \in \mathbb{R}^n$ and $\boldsymbol{\beta}_j \in \mathbb{R}^M$ represent the input and output weights of the $j$-th hidden node, respectively, $\boldsymbol{b}_j$ is the threshold of the $j$-th hidden node. The training processing is to obtain the optimal output weight matrix $\hat{\boldsymbol{\beta}}$, which can minimise the empirical error of the RWN model, i.e.,

$$\hat{\boldsymbol{\beta}} = \arg\min_{\boldsymbol{\beta}} \sum_{j=1}^{m} \left\| \boldsymbol{o}_i(\boldsymbol{\beta}) - \boldsymbol{y}_i \right\|_2^2 . \tag{9}$$

Therefore, the output weight matrix $\hat{\boldsymbol{\beta}}$ is calculated by,

$$\hat{\boldsymbol{\beta}}=\boldsymbol{H}^{\dagger}\boldsymbol{O}, \tag{10}$$

where $\boldsymbol{H}^{\dagger}$ stands for the Moore-Penrose generalised inverse of $\boldsymbol{H}$ [22], and $\boldsymbol{H}$ *is*,

$$\boldsymbol{H}=\begin{bmatrix} \phi(\boldsymbol{\omega}_1\boldsymbol{x}_1+b_1) & \cdots & \phi(\boldsymbol{\omega}_L\boldsymbol{x}_1+b_L) \\ \vdots & \ddots & \vdots \\ \phi(\boldsymbol{\omega}_1\boldsymbol{x}_m+b_1) & \cdots & \phi(\boldsymbol{\omega}_L\boldsymbol{x}_m+b_L) \end{bmatrix}, \tag{11}$$

and,

$$\boldsymbol{O}=[\boldsymbol{o}_1{}^{\mathrm{T}}, \boldsymbol{o}_2{}^{\mathrm{T}},\ldots, \boldsymbol{o}_m{}^{\mathrm{T}}]^{\mathrm{T}}\in \mathbb{R}^{m\times M}. \tag{12}$$

*2.4 PCA-RWN based combustion process monitoring*

As described in the previous sections, the colour and texture features are calculated from filtered flame images, as given in (3). In order to recognise combustion operation conditions, row vectors in score matrix $\boldsymbol{X}$ in (7), i.e. the features extracted by the PCA, are treated as the inputs of the RWN model. Assume the dimension of original feature vectors is $N$, the number of principal components is $n$, and the output dimension is 1, for a sample in $s$-th operation condition, the inputs and target outputs of the RWN model is expressed as,

$$\{(\boldsymbol{x}_i^{(n)}, y_i^{(n)}) \mid \boldsymbol{x}_i^{(n)}=\boldsymbol{d}_i\boldsymbol{P}_n \in \mathbb{R}^{n}, y_i^{(n)}=s \in \mathbb{R}\}_{n=1,s=1}^{N,\ S}, \tag{13}$$

where $S$ stands for the total number of combustion conditions.

*A. PCA-RWN based operation condition recognition*

A parallel model structure with $N$ irrelevant single RWN models is constructed using the different number of input vectors. The $n$-th RWN model in the model structure can be represented as,

$$\sum_{j=1}^{L}\beta_j^{(n)}\Phi(\boldsymbol{\omega}_j^{(n)}\boldsymbol{x}_i^{(\mathrm{n})^{\mathrm{T}}}+b_j^{(n)})=o_i, \tag{14}$$

where $\beta_j^{(n)}$, $\boldsymbol{\omega}_j^{(n)}$ and $b_j^{(n)}$ are the output weight, input weight and threshold of $j$-th hidden node in the $n$-th RWN model, respectively. $\{\boldsymbol{x}_i^{(n)}\}$ stand for the input vectors. All RWN models share the same outputs $\{o_i\}$, the number of hidden nodes $L$, and activation function $\Phi(.)$, $i$=1, …, $m$, $j$=1,…, $L$, $n$=1, …, $N$. The RWN models are built through the following steps,

- Calculate the loading matrices $\{\boldsymbol{P}_n\}$ with the different numbers of principal components, and initialise the input vectors $\{\boldsymbol{x}_i^{(n)}=\boldsymbol{d}_i\boldsymbol{P}_n\}$ and output vectors $\{o_i\}$, $i$=1, …, $m$, $n$=1, …, $N$.
- Assign randomly the input weights $\omega_j^{(n)}$ and thresholds $b_j^{(n)}$ of the $N$ single RWN models, respectively, $j$=1, …, $L$, $n$=1, …, $N$.
- Calculate the hidden layer output matrices $\boldsymbol{H}^{(n)}$ of the $N$ single RWN models, respectively, $n$=1, …, $N$.
- Calculate the output weights of the $N$ single RWN models as, $\hat{\boldsymbol{\beta}}^{(n)}=\boldsymbol{H}^{(n)^{\dagger}}\boldsymbol{O}$, $n$=1, …, $N$.
- Select the well-trained RWN with the optimal number of principal components and hidden nodes.

In order to make sure that the selected PCA-RWN model has satisfactory performance and robustness, $k$-fold cross validation [24] is used to determine the appropriate RWN model and the parameters of the PCA-RWN model. In the $k$-fold cross validation, the training samples are randomly split into $k$ mutually exclusive subsets (the folds) of equal size. The model is trained and tested for $k$ times, and for each time, the model is trained by $k$-1 subsets and tested by the rest. The cross-validation estimator, $E_{CV}$, which indicates the average error of operation condition recognition committed by the $n$-th PCA-RWN, is calculated by,

$$E_{CV}(L,\, n)=\frac{1}{m}\sum_{i=1}^{m}|o_i^{(n)}(\boldsymbol{\beta}^L)-y_i| \quad . \tag{15}$$

The optimal principal components $n_0$ and hidden nodes number $L_0$ are selected using,

$$[L_0,\, n_0]=\arg\min_{L,n}\left[E_{CV}(L,\, n)\right] \quad . \tag{16}$$

The final well-trained model is,

$$o_i^* := \varphi^*(\boldsymbol{x}_i) = \sum_{j=1}^{L_0} \hat{\beta}_j^{(n_0)} \Phi(\boldsymbol{\omega}_j^{(n_0)} \boldsymbol{x}_i^{\mathrm{T}} + b_j^{(n_0)}) \quad , \tag{17}$$

where $o_i^*$ stands for the final outputs of *i*-th training sample.

*B. State identification based on $T^2$ and SPE statistics*

$T^2$ and SPE are calculated and compared with their control limits to assess the state of the combustion, following the recognition of the operation condition. $T^2$ and SPE are defined as [25],

$$T_s^2 = \|\Lambda_{sn}^{-1/2} \boldsymbol{P}_s^{\mathrm{T}} \boldsymbol{x}\|_2^2 \le \delta_s^2 , \tag{18}$$

$$\mathrm{SPE}_s = \|\boldsymbol{x} - \boldsymbol{P}_s \boldsymbol{P}_s^{\mathrm{T}} \boldsymbol{x}\|_2^2 \le \chi_s^2 , \tag{19}$$

where $\Lambda_s$ is the diagonal matrix of eigenvalues of the corresponding condition, $\boldsymbol{P}_s$ is the loading matrix. $\delta_s^2$ stands for the $T_s^2$ statistic control limit of the *s*-th operation condition and $\chi_s^2$ is the control limit of $\mathrm{SPE}_s$. A detailed description of $\delta_s^2$ and $\chi_s^2$ calculations can be found in [19]. The statistics will be above the control limits if there are abnormalities, and vice versa, and therefore the monitoring of the combustion process state is achieved.

## 3. Results and discussion

*3.1 Experimental setup and test conditions*

In order to evaluate the proposed PCA-RWN model for monitoring the combustion conditions, experimental tests were carried out on a 250 $\mathrm{kW_{th}}$ air- and oxy-fuel CTF located at the UKCCSRC PACT Core Facilities. Fig. 2 shows the overview of the CTF and the installation of the flame imaging system. The CTF consists of a down fired single burner furnace with an inner diameter of 0.9 m. The burner, mounted on top of the rig inside the quarl section, is a scaled

version of a commercial Low-$NO_x$ burner with a primary annulus for introducing pulverised fuel and carrier gas. The swirled secondary and tertiary annuli are to deliver the rest of the oxidizer to ensure the completion of the combustion. The burner is also equipped with an internal air splitting system to control the secondary and tertiary air (SA/TA) ratio.

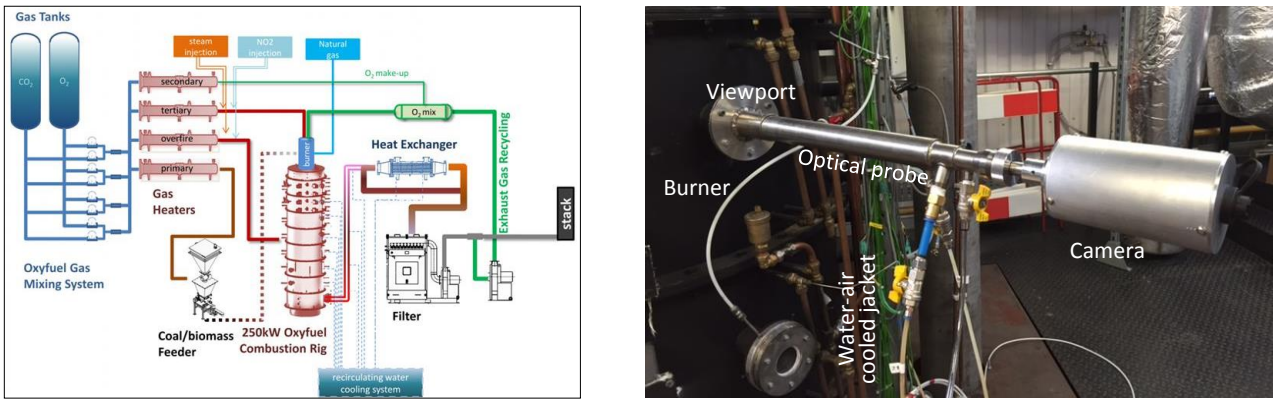


(a) Overview of the 250$kW_{th}$ CTF.

(b) Site installation of the flame imaging system.

Fig. 2 Experimental setup.

The flame imaging system used [1] consists of an optical probe (protected by a water-air cooled jacket) and an industrial RGB digital camera with a resolution of 256×320 pixels and a frame rate up to 200 frames per second. The probe was installed at the viewport on the section of the furnace. It is equipped with a 90° angle of view objective lens, which allows the burner quarl and primary reaction zone of flame to be fully visualized.

Two test programmes were conducted using the pulverised El Cerrejon coal. The ultimate and proximate analysis along with calorific value data of the coal tested are summarised in Table 1. During the tests, the fuel loading was maintained at the 200$kW_{th}$ firing rate, and target exit $O_2$ concentration was 3.5% on a dry basis. In the first test, three different primary air supplies were used, with the primary air flows of 18%, 20%, and 22% to the total air flow. In the second test, five different SA/TA split positions were examined, utilising the burner's internal SA/TA split

slide. At the initial SA/TA split position '0', all flow went through the secondary annulus, whereas with an increasing split position the SA/TA ratio decreases. Computational Fluid Dynamics (CFD) simulations were used to determine the SA/TA flows at the typically used split positions of 3 and 4 to be 48/55 and 45/55, respectively [26]. The detailed test programmes are illustrated in Table 2. Fig. 3 shows the flame images captured for different primary air flows under the furnace load of 200 kW and SA/TA split 3 whilst Fig. 4 presents the flame images for different SA/TA splitter positions under the furnace load of 200 kW and the primary air of 20%. Note, in this study, all the computations were carried out in Matlab R2015a environment in a personal computer with an i5-63317U processor, 1.7 GHz CPU and 4 GB RAM.

Table 1 Ultimate and proximate analysis and calorific value data of the El Cerrejon coal.

| Ultimate analysis (%, as received) | | Proximate analysis (%, as received ) | |
|---|---|---|---|
| Carbon | 73.57 | Fixed carbon | 54.92 |
| Hydrogen | 5.04 | Volatile matter | 37.84 |
| Oxygen (by diff.) | 11.31 | Ash | 1.43 |
| Nitrogen | 2.47 | Moisture | 5.81 |
| Sulphur | 0.37 | | |
| Gross calorific value (MJ/kg) | | 30.79 | |
| Net calorific value (MJ/kg) | | 29.57 | |

Table 2 Test programmes.

| Test | Primary air (%) | SA/TA split position (SA/TA ratio) |
|---|---|---|
| 1 | 18<br>20<br>22 | 3 (48/55) |
| 2 | 20 | 1<br>2<br>3 (48/55)<br>4 (45/55)<br>5 |

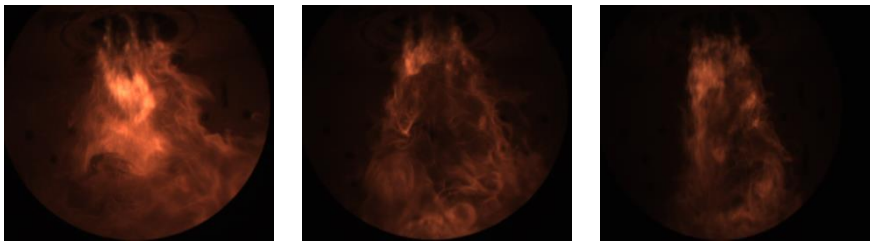

18% 20% 22%

Fig. 3 Flame images for different primary air flows under the SA/TA split of 3 (48/55).

1 2 3 4 5

Fig. 4 Flame images for different SA/TA splits under the primary air of 20%.

*3.2 Combustion process monitoring for different primary air flows*

In Test 1 (Table 2), flame image features calculated from 2800 flame images for each condition, as shown in Table 2, were used as the training data of the proposed PCA-RWN model. 14-fold cross validation was introduced to select the proper parameters of the PCA-RWN model to ensure satisfactory performance of the condition recognition, i.e. the number of principal components and hidden nodes. The cross-validation estimator of 14 trials is shown in Fig. 5.

It can be seen that the cross-validation estimator of the PCA-RWN is strongly related to the numbers of principal components and hidden nodes. With the increase of hidden node number, the cross-validation estimator decreases in general. The cross-validation estimator remains constant around 0.13 with slight disturbances when the number of hidden nodes reaches to 20. In addition, it decreases with the number of principal components and achieves the bottom when the principal component number is 8 with 25 hidden nodes, with which the optimal performance of the proposed PCA-RWN is reached. Then, the cross-validation estimator decreases when the

number of principal components is in the range of 9 to 17, which is possibly because the increased principal components may introduce more noise and abnormalities. In the PCA-RWN model studied, the optimal number of principal components is 8 and the number of hidden nodes is 25.

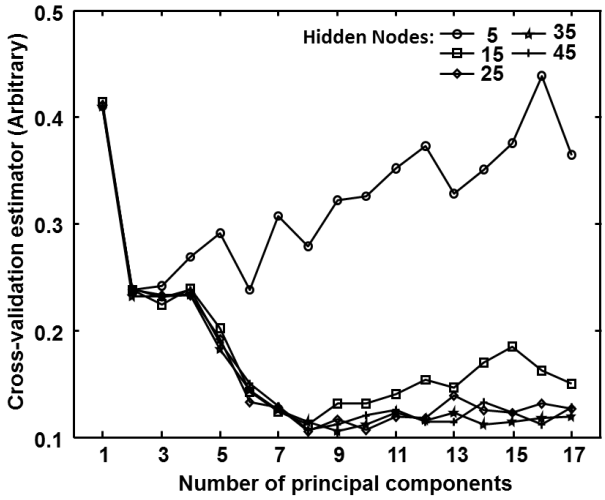


Fig. 5 Cross-validation estimator of the PCA-RWN with different number of hidden nodes and principal components for the primary air flow test.

Colour and texture features for a total of 600 flame images evenly distributed under three conditions were employed as the test data of the PCA-RWN model, including 100 abnormal samples for the primary air of 18%, which were selected from abnormal events. Figs. 6 and 7 show the results for the operation condition recognition and state monitoring using the PCA-RWN for different primary air flows.

It can be seen from Fig. 6 that the PCA-RWN model can recognise the combustion operation conditions with a success rate up to 99%. There are some false recognitions which occur under the primary air of 18% and 20%, but, from a practical engineering perspective, these failures in the condition recognitions are acceptable. Following recognising the operation conditions, the $T^2$ and SPE statistics are calculated for monitoring the state of the corresponding operation (Fig. 7). When the primary air ratio is 18%, the $T^2$ and SPE are under the control limits for the first 100

samples. The $T^2$ and SPE are above the control limits for sample 101-200, indicating these flames are under an abnormal state. In the primary air of 20% and 22%, there is no abnormal state. The results have suggested that the proposed PCA-RWN can effectively recognise the operation conditions and the $T^2$ and SPE are useful to detect the abnormalities.

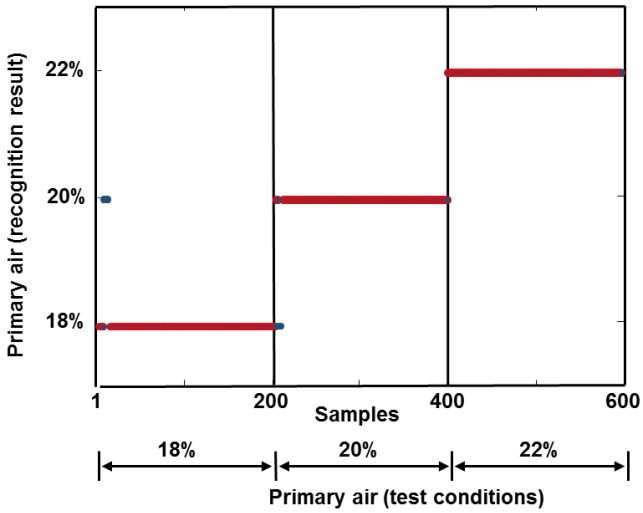


Fig. 6 Operation condition recognition under different primary air flows.

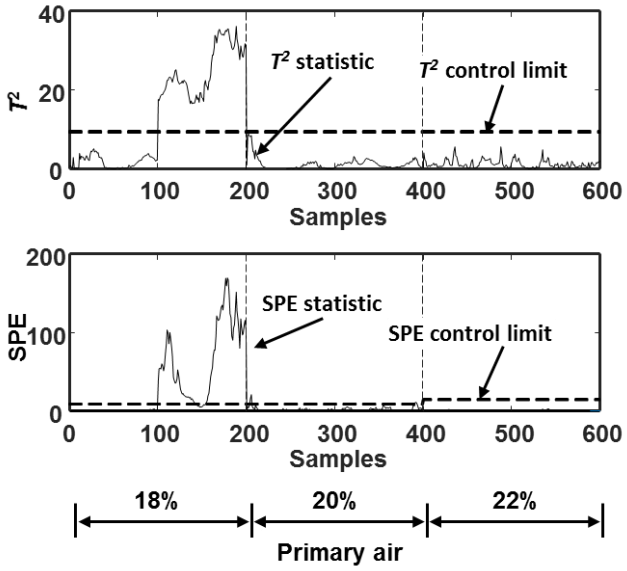


Fig. 7 State monitoring under different primary air flows.

*3.3 Combustion process monitoring for different SA/TA ratios*

In Test 2 (Table 2), flame image features extracted from 2800 samples (per condition) from SA/TA splits 1 to 5 were used to train the PCA-RWN model. Fig. 8 shows the results of the 14-fold cross validation estimator for different PCA-RWN parameters. In this test, the trend of cross-validation estimator is similar to that in Test 1, and the optimal number of principal components and hidden nodes is 11 and 65, respectively.

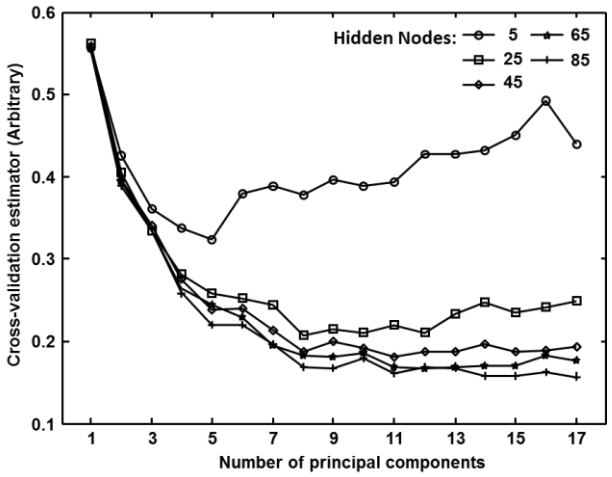


Fig. 8 Cross-validation estimator of the PCA-RWN with the different number of hidden nodes and principal components for the SA/TA split test.

In the test stage, a total of 1000 flame images acquired from five SA/TA splits (200 per operation condition) with 100 abnormal samples in SA/TA split 1 and SA/TA split 4 are used as the test data. Fig. 9 shows the condition recognition using the PCA-RWN for different SA/TA splits. It can be seen that the false condition recognitions are more than that in Test 1. The reason is that the flames under the different SA/TA splits are very similar, which makes it more difficult to recognise the operation condition with a high success rate. The PCA-RWN model can distinguish the conditions with a success rate about 93%. Some false recognition results may lead to false alarms that lead the $T^2$ or SPE above the control limits. Fig. 10 shows the results of the state monitoring. The $T^2$ and SPE are above the control limits from 1-60 and 701-800 where the abnormalities occurr.

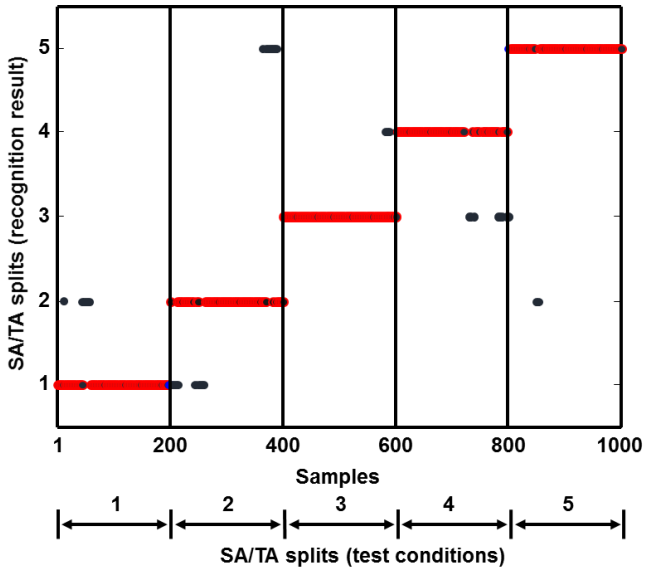


Fig. 9 Operation condition recognition for different SA/TA splits.

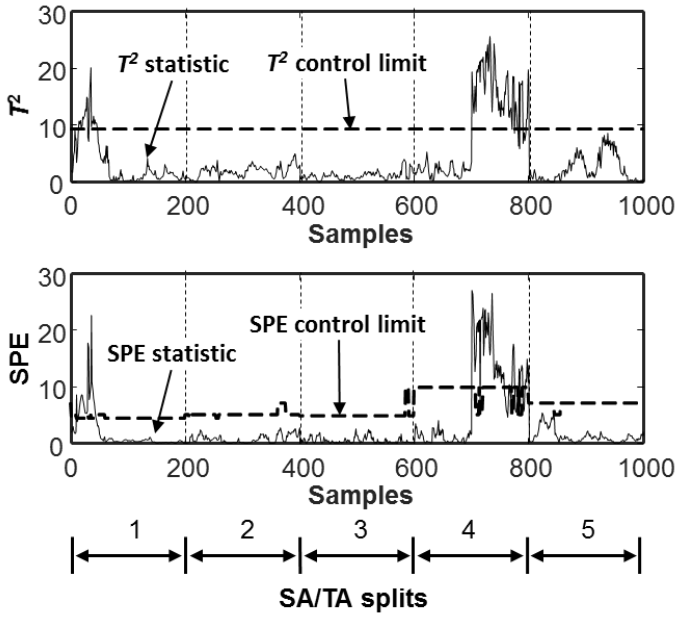


Fig. 10 State monitoring for different SA/TA splits.

*3.4 Flame oscillation frequency*

As the flame oscillation is closely associated with combustion stability, and consequently combustion efficiency and pollutant emissions, the oscillation frequency of flame has widely been studied [27, 28]. The oscillation frequency of the flame can therefore be used to assess the effectiveness of the proposed PCA-RWN model. The oscillation frequency of a flame is defined

as the weighted average frequency of the flame signal over the entire frequency range, where the weighting factor is the power density of the individual frequency component [28]. In this study, the oscillation frequency of the flame was calculated using the average grey-values of the flame images. The flame images which were used as the training data for each condition (2800 images per condition) were equally divided into 14 groups in sequence and the oscillation frequency range of these 14 flame image groups are considered to be the appropriate range for normal flames. Figs. 11(a) and 11(b) show that the averaged oscillation frequencies and their standard deviations of the flames that were used as training data, as well as the oscillation frequencies of flames that were also used as the test data. The flame oscillation frequencies of the normal states are included in the frequency range of the training data. The oscillation frequencies of the flame under abnormal states are beyond the range, such as under the primary air of 18%, SA/TA splits 1 and 4. These results are consistent with that derived from the PCA-RWN model, suggesting that the proposed multi-mode process monitoring approach is effective for recognising the normal and abnormal states of combustion process.

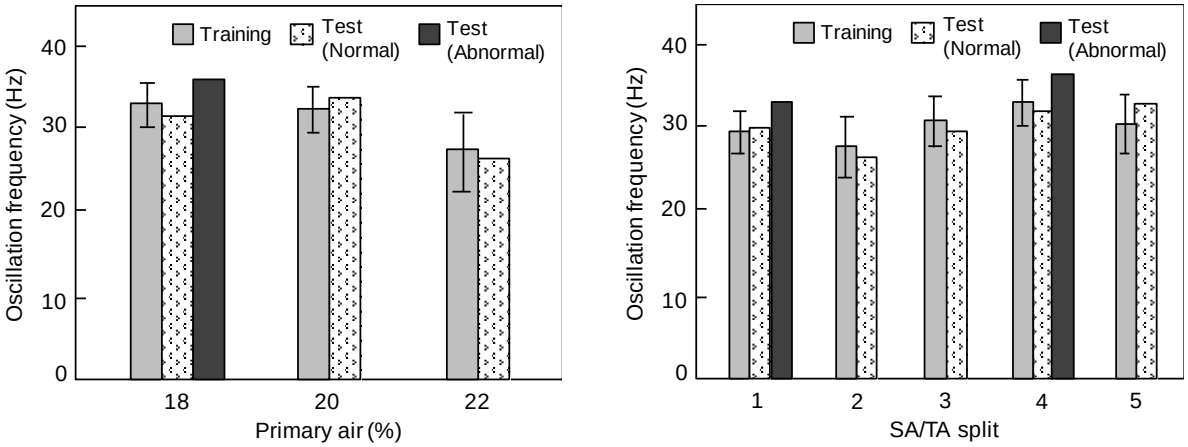


(a) Different primary air flows. (b) Different SA/TA splits.

Fig. 11 Flame oscillation frequency.

*3.5 Comparison of the PCA-RWN with other machine learning classifiers*

To further evaluate the performance of the proposed PCA-RWN model for multi-mode combustion process monitoring, the recognition success rate (i.e. the ratio of correctly recognised flame images and the total number of images) and the system time for the training process of the model are compared with that of other machine learning classifiers used widely in mode recognition, including Kernel Support Vector Machine (KSVM) [29], Neural Network (NN) [30] and k-Nearest Neighbour classifier (kNN) [31]. A total of 2000 images are randomly selected from the test data set and equally split into 10 groups for different operation conditions. The success rate of condition recognition and the training time required for the 10 groups are summarised in Table 3. As can be seen, the PCA-RWN performs the best among the models in terms of the average recognition success rate and the training time, which means that the robustness of the PCA-RWN model is high enough for different test flame images. The reduced system time of the training process also allows the model to be updated swiftly.

Table 3 Comparison of PCA-RWN with other machine learning classifiers.

| | Test 1 | | Test 2 | |
|---|---|---|---|---|
| | Success rate (%) | Training time (s) | Success rate (%) | Training time (s) |
| PCA-RWN | **92.9±0.9** | **0.11±0.07** | **91.3±1.2** | 0.48±0.04 |
| PCA-KSVM | 92.7±0.7 | 10.08±0.82 | 87.1±0.3 | 31.94±1.86 |
| PCA-NN | 91.7±1.5 | 5.76±3.11 | 75.1±2.6 | 29.97±9.37 |
| PCA-KNN | 75.2±0.8 | 0.34±0.69 | 70.9±0.6 | 0.32±0.09 |

## 4. Conclusions

In this study, a multi-mode combustion process monitoring technique based on flame imaging, PCA and RWN principles has been proposed and its applicability has been examined in an industrial combustion environment. Flame images acquired from the digital imaging system are denoised using a moving average filter. A global PCA-RWN model has been built to extract

colour and texture features which are then used to recognise the combustion operation condition. The cross-validation has been proved to be effective to select the optimal parameters of the PCA-RWN model. The $T^2$ and SPE statistics have been calculated for identifying the combustion state of the corresponding conditions. The proposed method has been evaluated on an industrial-scale pulverised coal fired combustion test facility under different operation conditions. The results have demonstrated that, for both variable primary air flow and SA/TA ratio operation conditions, the condition recognition success rate of the PCA-RWN model is over 91%, which is at least 4% higher than that of other machine learning classifiers with a reduced training time. The $T^2$ and SPE indices have also been proved to be effective and reliable in detecting the abnormalities. It can therefore be concluded that the proposed PCA-RWN model for multi-mode process monitoring is promising for recognising the condition and state of practical combustion processes. The PCA-RWN can also potentially be applied to recognise untrained conditions so as to achieve completely unsupervised combustion process monitoring.

## Acknowledgements

The authors acknowledge that the UKCCSRC PACT Facilities, funded by the Department for Business, Energy & Industrial Strategy and the Engineering and Physical Sciences Research Council, have been used for the experimental work reported in this publication. The China Scholarship Council is also acknowledged for providing a fellowship to Xiaojing Bai for studying at the University of Kent.

## References

[1] Sun D, Lu G, Zhou H, Yan Y. Condition monitoring of combustion processes through flame imaging and kernel principal component analysis. Combust. Sci. Technol. 2013; 185: 1400-13.

[2] Sun D, Lu G, Zhou H, Yan Y, Liu S. Quantitative assessment of flame stability through image processing and spectral analysis. IEEE Trans. Instrum. Meas. 2015; 64: 3323-33.

[3] Li W, Wang D, Chai T. Flame image-based burning state recognition for sintering process of rotary kiln using heterogeneous features and fuzzy integral. IEEE Trans. Ind. Inf. 2012; 8: 780-90.

[4] Chen J, Hsu TY, Chen CC, Cheng YC. Online predictive monitoring using dynamic imaging of furnaces with the combinational method of multiway principal component analysis and hidden Markov model. Ind. Eng. Chem. Res. 2011; 50: 2946-58.

[5] Chen H, Zhang J, Hu H, Zhang X. Recognition of sintering state in rotary kiln using a robust extreme learning machine. In: Proceedings of International Joint Conference on Neural Networks. 2014 July 6 - 11; Beijing, China. IEEE; p. 2564-70.

[6] Wang J, Ren X. GLCM based extraction of flame image texture features and KPCA-GLVQ recognition method for rotary kiln combustion working conditions. Int. J. Autom. Comput. 2014; 11: 72-77.

[7] Shang C, Yang F, Gao X, Huang X, Suykens JA, Huang D. Concurrent monitoring of operating condition deviations and process dynamics anomalies with slow feature analysis. AlChE J. 2015; 61: 3666-82.

[8] Ma H, Hu Y, Shi H. A novel local neighborhood standardization strategy and its application in fault detection of multimode processes. Chemometr. Intell. Lab. 2012; 118: 287-300.

[9] Wang G, Liu J, Zhang Y, Li Y. A novel multi-mode data processing method and its application in industrial process monitoring. J. Chemom. 2015; 29: 126-38.

[10] Lee YH, Jin HD, Han C. On-line process state classification for adaptive monitoring. Ind. Eng. Chem. Res. 2006; 45: 3095-107.

[11] Ma Y, Shi H, Ma H, Wang M. Dynamic process monitoring using adaptive local outlier factor. Chemometr. Intell. Lab. 2013; 127: 89-101.

[12] Ge Z, Song Z. Online monitoring of nonlinear multiple mode processes based on adaptive local model approach. Control Eng. Pract. 2008; 16: 1427-37.

[13] Feital T, Kruger U, Dutra J, Pinto JC, Lima EL. Modeling and performance monitoring of multivariate multimodal processes. AlChE J. 2013; 59: 1557-69.

[14] Yang Y, Ma Y, Song B, Shi H. An aligned mixture probabilistic principal component analysis for fault detection of multimode chemical processes. Chinese J. Chem. Eng. 2015; 23: 1357-63.

[15] Qiu T, Yan Y, Lu G. A new edge detection algorithm for flame image processing. In: Proceedings of Instrumentation and Measurement Technology Conference. 2011 May 10 - 12; Hangzhou, China. IEEE; p. 1-4.

[16] Kim BS, Moon YS, Kim J. Noise control boundary image matching using time-series moving average transform. In: Proceedings of International Conference on Database and Expert Systems Applications. 2008 September 1 - 5; Turin, Italy. Springer Berlin Heidelberg; p. 362-375.

[17] Haralick RM, Shanmugam K, Dinstein IH. Textural features for image classification. IEEE Trans. Syst., Man Cybern. 1973; 6: 610-21.

[18] Cui Y, Dong H, Zhou E. An early fire detection method based on smoke texture analysis and discrimination. In: Proceedings of Congress on Image and Signal Processing. 2008 May 27 - 30; Hainan, China. IEEE; p. 95-99.

[19] Qin SJ. Statistical process monitoring : basics and beyond. J. Chemom. 2003: 480-502.

[20] Pao YH, Park GH, Sobajic DJ. Learning and generalization characteristics of the random vector functional-link net. Neurocomputing. 1994; 6: 163-80.

[21] Huang GB, Zhu QY, Siew CK. Extreme learning machine: theory and applications. Neurocomputing. 2006; 70: 489-501.

[22] Cao F, Tan Y, Cai M. Sparse algorithms of Random Weight Networks and applications. Expert Syst. Appl. 2014; 41: 2457-62.

[23] He YL, Wang XZ, Huang JZ. Fuzzy nonlinear regression analysis using a random weight network. Inform. Sciences. 2016; 364: 222-40.

[24] Kohavi R. A study of cross-validation and bootstrap for accuracy estimation and model selection. In: Proceedings of International Joint Conference on Artificial Intelligence. 1995 August 20 - 25; Quebec, Canada. Morgan Kaufmann Publishers Inc. San Francisco, CA, USA; p. 1137-45.

[25] Ge Z, Song Z. Distributed PCA model for plant-wide process monitoring. Ind. Eng. Chem. Res. 2013; 52: 1947-57.

[26] Black AJ. Oxy-fuel combustion for carbon capture using computational fluid dynamics. 2014; PhD thesis.

[27] Xu L, Yan Y. An improved algorithm for the measurement of flame oscillation frequency. IEEE Trans. Instrum. Meas. 2007; 56: 2087-93.

[28] Huang Y, Yan Y, Lu G, Reed A. On-line flicker measurement of gaseous flames by image processing and spectral analysis. Meas. Sci. Technol. 1999; 10: 726-33.

[29] Han H, Cao Z, Gu B, Ren N. PCA-SVM-based automated fault detection and diagnosis (AFDD) for vapor-compression refrigeration systems. HVAC&R Research. 2010; 16: 295-313.

[30] Neumann DE. An enhanced neural network technique for software risk analysis. IEEE Trans. Software Eng. 2002; 28: 904-12.

[31] Cunningham P, Delany SJ. k-Nearest neighbour classifiers. Dublin: Artificial Intelligence Group 2007: UCD-CSI-2007-4.